

Published in final edited form as:

Cancer Res. 2008 April 1; 68(7): 2329–2339. doi:10.1158/0008-5472.CAN-07-5167.

## Loss of E-Cadherin Promotes Ovarian Cancer Metastasis via $\alpha_5$ -Integrin, which Is a Therapeutic Target

Kenjiro Sawada<sup>1</sup>, Anirban K. Mitra<sup>1</sup>, A. Reza Radjabi<sup>1</sup>, Vinay Bhaskar<sup>6</sup>, Emily O. Kistner<sup>2</sup>, Maria Tretiakova<sup>3</sup>, Sujatha Jagadeeswaran<sup>1</sup>, Anthony Montag<sup>3</sup>, Amy Becker<sup>1</sup>, Hilary A. Kenny<sup>1</sup>, Marcus E. Peter<sup>4,5</sup>, Vanitha Ramakrishnan<sup>6</sup>, S. Diane Yamada<sup>1</sup>, and Ernst Lengyel<sup>1,5</sup>

<sup>1</sup>Department of Obstetrics and Gynecology/Section of Gynecologic Oncology, University of Chicago, Chicago, Illinois

<sup>2</sup>Department of Health Studies, University of Chicago, Chicago, Illinois

<sup>3</sup>Department of Pathology, University of Chicago, Chicago, Illinois

<sup>4</sup>Department of Ben May Department for Cancer Research, University of Chicago, Chicago, Illinois

<sup>5</sup>Department of Committee on Cancer Biology, University of Chicago, Chicago, Illinois

<sup>6</sup>PDL BioPharma, Fremont, California

### Abstract

E-cadherin loss is frequently associated with ovarian cancer metastasis. Given that adhesion to the abdominal peritoneum is the first step in ovarian cancer dissemination, we reasoned that down-regulation of E-cadherin would affect expression of cell matrix adhesion receptors. We show here that inhibition of E-cadherin in ovarian cancer cells causes up-regulation of  $\alpha_5$ -integrin protein expression and transcription. When E-cadherin was blocked, RMUG-S ovarian cancer cells were able to attach and invade more efficiently. This greater efficiency could, in turn, be inhibited both *in vitro* and *in vivo* with an  $\alpha_5\beta_1$ -integrin–blocking antibody. When E-cadherin is silenced,  $\alpha_5$ -integrin is up-regulated through activation of an epidermal growth factor receptor/FAK/Erk1–mitogen-activated protein kinase–dependent signaling pathway and not through the canonical E-cadherin/ $\beta$ -catenin signaling pathway. In SKOV-3ip1 ovarian cancer xenografts, which express high levels of  $\alpha_5$ -integrin, *i.p.* treatment with an  $\alpha_5\beta_1$ -integrin antibody significantly reduced tumor burden, ascites, and number of metastasis and increased survival by an average of 12 days when compared with IgG treatment ( $P < 0.0005$ ).  $\alpha_5$ -Integrin expression was detected by immunohistochemistry in 107 advanced stage ovarian cancers using a tissue microarray annotated with disease-specific patient follow-up. Ten of 107 tissues (9%) had  $\alpha_5$ -integrin overexpression, and 39% had some level of  $\alpha_5$ -integrin expression. The median survival for patients with high  $\alpha_5$ -integrin levels was 26 months versus 35 months for those with low integrin expression ( $P < 0.05$ ). Taken together, we have identified  $\alpha_5$ -integrin up-regulation as a molecular mechanism by which E-cadherin loss promotes tumor progression, providing an explanation for how E-cadherin loss increases metastasis. Targeting this integrin could be a promising therapy for a subset of ovarian cancer patients.

## Introduction

Most ovarian cancers are of epithelial origin, arising from a single layer of simple epithelial cells that covers the surface of the ovary (1,2). Once an ovarian epithelial cell undergoes transformation, it detaches easily from the underlying basement membrane and can metastasize throughout the peritoneal cavity, carried by the flow of peritoneal fluid. Although the precise regulation of i.p. spread of ovarian cancer is unknown, we are aware that changes in the expression of cell-cell adhesion molecules make the cancer cells prone to exfoliation. One of the molecules critical for adhesion between neighboring epithelial cells is E-cadherin, a membrane glycoprotein located at cell adherens junctions (3,4). In ovarian cancer, E-cadherin expression in the cancer cells floating in ascites and at metastatic sites is lower than in the primary ovarian tumor. Moreover, ovarian cancer cells with low E-cadherin expression are more invasive (5), and the absence of E-cadherin expression in ovarian cancers predicts poor patient survival when compared with ovarian tumors that express E-cadherin (6). Upon contact of ovarian cancer cells with the extracellular matrix, E-cadherin is posttranslationally modified and the ectodomain is shed in a matrix metalloproteinase (MMP)-dependent manner (7). Whereas many studies clearly show that E-cadherin loss plays an important role in tumor biology by weakening cell-cell adhesion, they do not explain how E-cadherin loss promotes metastasis. Given that the adhesion of ovarian cancer cells to the mesothelial cells, which line the abdominal cavity, is the first step of ovarian cancer metastasis (1), we reasoned that loss of E-cadherin and weakening of cell-cell adhesion would affect expression of other adhesion molecules which are necessary for ovarian cancer metastasis. Indeed, several studies have shown the importance of CD44 and integrins for the adhesion of ovarian cancer cells (8,9).

Therefore, to test the hypothesis that E-cadherin regulates adhesion molecules, we inhibited E-cadherin expression and found significant up-regulation of  $\alpha_5$ -integrin, which in turn, acts to mediate adhesion to the peritoneal cavity *in vitro* and *in vivo*. In further support of the role of  $\alpha_5\beta_1$ -integrin in metastasis, inhibition of  $\alpha_5\beta_1$ -integrin reduced i.p. tumor spread and increased survival in two xenograft mouse models of ovarian cancer, identifying the inhibition of  $\alpha_5\beta_1$ -integrin as a potential new therapeutic target.

## Materials and Methods

### Reagents and cell lines

Anti-CD44 (515), FAK (77), and E-cadherin (36) monoclonal antibodies, collagen type 1, fibronectin, and vitronectin were purchased from BD Biosciences. The blocking antibody against  $\alpha_5\beta_1$ -integrin (IIA1) was initially purchased from BD Biosciences and then provided for the *in vivo* experiments (Fig. 4) by PDL BioPharma, Inc..  $\beta_1$ -integrin (P5D2) and  $\alpha_2$ -integrin (PIH5) were purchased from Santa Cruz Biotechnology. Antibodies against  $\alpha_5$ -integrin (polyclonal),  $\beta_3$ -integrin (B3A),  $\beta_4$ -integrin (3E1),  $\alpha_V\beta_3$ -integrin (LM609),  $\alpha_V\beta_5$ -integrin (PIF6), and  $\alpha_V\beta_6$ -integrin (10D5) were obtained from Chemicon. Anti-phosphorylated specific FAK (Tyr<sup>397</sup>) antibody was obtained from Biosource. Horseradish peroxidase-conjugated secondary antibodies were obtained from Cell Signaling. Anti-mouse  $\beta$ -actin (CP01) antibody was purchased from EMD Bioscience. Lipofectamine 2000, TRIzol, R-phycoerythrin (PE) goat anti-mouse IgG were purchased from Invitrogen. The human ovarian cancer cell lines CAOV-3 and OVCAR-5 were purchased from American Type Culture Collection. OVMZ-6 cells were provided by Dr. Volker Möbus (Hospital Frankfurt-Höchst). SKOV-3ip1 and HEYA8 were from Dr. Gordon B. Mills (M.D. Anderson Cancer Center) and first described by Dr. Dihua Yu. A2780 cells were from Dr. Poruchynsky (National Cancer Institute). RMUG-L and RMUG-S cells (10) were kindly provided by Dr. Samuel Mok (Brigham and Women, Harvard Medical School).

### Small interfering RNA knockdown of E-cadherin

The E-cadherin small interfering RNA (siRNA; ID146381, Ambion, Inc.; ref. 11) was transiently transfected into RMUG-S cells using Lipofectamine 2000. An siRNA concentration of 40 nmol/L was determined to be optimal, and a seeding cell count of  $5 \times 10^5$  cells per transfection well was used. Controls included a glyceraldehyde-3-phosphate dehydrogenase siRNA to confirm transfection efficiency and a scrambled siRNA sequence as negative control.

### Flow cytometry

Cells suspended in DMEM with 10% fetal bovine serum were incubated with the indicated primary monoclonal antibodies (1:250) for 30 min at 4°C followed by PE-labeled secondary antibody (Invitrogen) for 30 min at 4°C. After washing the cells thrice with 1% bovine serum albumin (BSA)/PBS, cells were resuspended in 500  $\mu$ L of 1% BSA/PBS. Isotypic mouse IgG was used as a negative control. Surface expressions of integrins and CD44 were measured with a FACS Calibur (Becton Dickinson; ref. 12).

### Western blot analysis

Cells ( $5 \times 10^5$ ) were plated onto six-well plates and lysed with radioimmunoprecipitation assay buffer [150 mmol/L NaCl, 50 mmol/L Tris-HCl (pH 7.5), 1% deoxycholate, 0.1% SDS, 1% Triton X-100, 1 mmol/L phenylmethylsulfonyl fluoride, 1 mmol/L NaOVO<sub>4</sub>, protease inhibitor cocktail; 1:1000, Sigma]. Lysate (15  $\mu$ g) was separated by 10% SDS-PAGE and transferred to nitrocellulose membranes which was incubated with the primary antibody [E-cadherin (BD Biosciences), 1:2,500 in 5% milk;  $\alpha_5$ -integrin (Chemicon), 1:5,000 in 5% BSA; FAK (BD Biosciences), 1:1,000 in 5% milk; p-FAK (Biosource), 1:2,000 in 5% BSA; actin, 1:10,000 in 5% milk] and then with a secondary horseradish peroxidase-conjugated IgG. The proteins were visualized with enhanced chemiluminescence.

Primary human peritoneal mesothelial cells were grown for 3 d and then removed from culture plates with 20 mmol/L NH<sub>4</sub>OH, followed by extensive washing. The extra cellular matrix was extracted using 50 mmol/L Tris-HCl (pH 6.8), 2% SDS, 0.1% bromophenol blue, 10% glycerol, 8 mol/L urea, and 100 mmol/L 2-mercaptoethanol and separated by SDS-PAGE (4–20% gradient) for Western blot analysis.

### Real-time PCR

Real-time quantitative reverse transcription-PCR (RT-PCR) was performed using the Prism7500 TaqMan PCR detector with the following probes:  $\alpha_5$ -integrin (Hs01547690\_g1) and glyceraldehyde-3-phosphate dehydrogenase (GAPDH; Hs00266705\_g1; Applied Biosystems). RNA was extracted using TRIzol and was transcribed into cDNA using high-capacity cDNA kit (Applied Biosystems). Relative levels of mRNA gene expression were calculated using the  $2^{-\Delta\Delta C_t}$  method as described (13).

### Transient transfections

The luciferase reporter construct pGL3 containing the promoter region of the human  $\alpha_5$ -integrin (14) subunit gene was kindly provided by Dr. Ritzenthaler (Emory University). Four hundred nanograms were transfected into  $1 \times 10^5$  cells using Lipofectamine 2000. To measure  $\beta$ -catenin-LEF/T-cell factor (TCF)-mediated transcription, reporter constructs with four consecutive wild-type (wt; TOPFLASH) or mutant (FOPFLASH) TCF binding sites were transfected. After E-cadherin siRNA transfection,  $1 \times 10^5$  RMUG-S cells were seeded in a 12-well plate and transiently transfected with 400 ng of either TOPFLASH or FOPFLASH firefly luciferase reporter and 40 ng of pRL-TK *Renilla* luciferase. Cells were lysed and analyzed using the Dual-Luciferase Reporter Assay System (Promega). Firefly luciferase values were normalized to *Renilla* luciferase values.

## Adhesion assays

To determine adhesion to the three-dimensional omental culture, primary human mesothelial cells and fibroblasts were isolated from the omentum as described (15). Specimens of human omentum were obtained from patients undergoing surgery for benign conditions at the University of Chicago. The three-dimensional omental culture was assembled by plating 2,000 primary fibroblast cells mixed with 0.5  $\mu\text{g}$  of collagen I in 96-well culture plates. After solidification, 10,000 primary mesothelial cells were added to the culture and incubated at 37°C until a confluent layer of mesothelial cells formed. SKOV-3ip.1 cells were treated with different blocking/neutralizing antibodies (mIgG 100  $\mu\text{g}/\text{mL}$ ,  $\alpha_5$ -integrin 10  $\mu\text{g}/\text{mL}$ ,  $\alpha_V\beta_3$ -integrin 10  $\mu\text{g}/\text{mL}$ ,  $\alpha_V\beta_5$ -integrin 5  $\mu\text{g}/\text{mL}$ ,  $\alpha_V\beta_6$ -integrin 100  $\mu\text{g}/\text{mL}$ ,  $\beta_3$ -integrin 10  $\mu\text{g}/\text{mL}$ ), control IgG, or not treated for 18 h. The SKOV-3ip.1 cells were fluorescently labeled with CMFDA (Invitrogen) at 37°C for 30 min in serum-free media, recovered for 30 min in serum-containing media, and washed twice with serum-free media. Adhesion was allowed to proceed for 4 h; cells were washed with PBS and fixed with 10% formalin. The number of adhesive cells was quantified by measuring the fluorescence intensity with a fluorescence spectrophotometer (Synergy HT) and use of a standard curve.

For the *in vitro* adhesion assay to ECM components, ovarian cancer cells were fluorescently labeled with 10  $\mu\text{mol}/\text{L}$  CMTPX and plated in a 96-well plate precoated with collagen type 1 (50  $\mu\text{g}/\text{mL}$ ), fibronectin (5  $\mu\text{g}/\text{mL}$ ) or vitronectin (5  $\mu\text{g}/\text{mL}$ ) and treated with IIA1 antibody (10  $\mu\text{g}/\text{mL}$ ) or an equivalent volume of a control mouse IgG. After incubation for 1 h at 37°C, cells were washed thrice and fixed with 4% formaldehyde in PBS. The number of adhesive cells was quantified by measuring fluorescent intensity (excitation, 590 nm; emission, 620 nm). Adhesion assays were run in triplicate.

To determine *in vivo* cell adhesion to the peritoneum, SKOV-3ip.1 cells were fluorescently labeled, and  $2 \times 10^6$  cells were injected into the peritoneal cavity of female athymic nude mice with IIA1 antibody (100  $\mu\text{g}/\text{mL}$ ) or control IgG. After 4 h, mice were sacrificed, and the full omentum was excised and placed in a 24-well culture plate. Adherent cells were lysed with NP40, and fluorescence was measured.

## Proliferation assay

The proliferation of ovarian cancer cells was measured using a fluorescence dye which shows strong fluorescence enhancement when bound to nucleic acids (CyQuant cell proliferation assay kit, Molecular Probes). SKOV-3ip.1 cells ( $3 \times 10^3$ ) were seeded in 96-well plates in the presence of IIA1 (10  $\mu\text{g}/\text{mL}$ ) or mouse IgG. At the indicated time points, cells were washed with serum-free medium and frozen at  $-80^\circ\text{C}$ . Cells were lysed with a buffer containing the fluorescent dye, and fluorescence was measured using a Synergy HT (Bio-Tek) multiwell fluorescence plate reader with excitation at 485 nm and emission at 530 nm.

## Matrigel invasion assay

*In vitro* cellular invasion was assayed by determining the ability of cells to invade through a synthetic basement membrane (Matrigel, BD Biosciences). Briefly, polycarbonate filters (8  $\mu\text{m}$  pore size) coated with 20  $\mu\text{g}$  Matrigel were placed in a modified Boyden chamber. RMUG-S cells ( $1 \times 10^5$  per well) were plated to the top chamber in serum-free media and incubated with serum-containing media as a chemoattractant in the bottom chamber. Cells were then incubated at 37°C and allowed to invade through the Matrigel barrier for 24 h. After incubation, filters were fixed and stained with Giemsa. Noninvading cells were removed using a cotton swab, and invading cells on the underside of the filter were enumerated using an inverted microscope. Experiments were performed in triplicate with a minimum of 10 grids (100 $\times$  magnification) per filter counted.

## Plasminogen and gelatin zymogram

These were done as described (16,17).

## Confocal microscopy

After the transfection of the E-cadherin siRNA, RMUG-S cells were plated in eight-well chamber slides coated with fibronectin (5  $\mu\text{g}/\text{mL}$ ) and then cultured under serum-free conditions for 24 h. After incubation, cells were fixed with 4% paraformaldehyde in PBS for 30 min and stained with mouse anti-E-cadherin (BD Biosciences; 1:100) or mouse anti- $\beta$ -catenin (BD Biosciences; 1:50) at 4°C overnight. After washing, samples were incubated with Alexa Fluor 555-labeled goat anti-mouse IgG or Alexa Fluor 488-labeled goat anti-mouse IgG (Molecular Probe; 1:1000) and finally stained with 4',6-diamidino-2-phenylindole (DAPI). The samples were analyzed using a Leica SP2 A OBS laser scanning confocal microscope (Leica).

## Orthotopic *in vivo* model

SKOV-3ip1 cells ( $1 \times 10^6$ ), verified to be without pathogens, were suspended as single cells in a volume of 500  $\mu\text{L}$  of PBS and injected i.p. into female athymic nude mice. One week after injection of the cancer cells, the  $\alpha_5$ -integrin-blocking antibody (IIA1), nonspecific mouse IgG (ChromePure mouse IgG), or an equivalent volume of PBS was injected i.p. twice a week for a total of 4 wk of treatment. Mice were assessed daily for general health and development of ascites. Twice weekly, their weight was measured and abdominal circumference was determined. For the two survival studies (SKOV-3ip.1, HeyA8), mice were sacrificed upon evidence of distress. After sacrifice, ascites was quantified, the number of metastases was counted and carefully dissected, and the removed tumor was then weighed. Procedures involving animals were approved by the Institutional Committee on Animal Care, University of Chicago.

Tumor tissue was fixed in 10% PBS-buffered formalin and embedded in paraffin. Angiogenesis was detected in tumor tissue with anti-goat CD31 antibody (Santa Cruz) at 1:100 dilution and the Envision avidin-biotin-free detection system (DAKO). Five fields were arbitrarily selected, and the number of vessels was assessed by two independent pathologists. Cell proliferation was detected immunohistochemically by staining using the rabbit Ki-67 antibody (Sp6, LabVision) at 1:300 dilution. Ten fields were arbitrarily selected, and the ratio of Ki-67-positive nuclei in tumor cells counted using the Cellular Image Analysis System (ACIS).

## Patients, tissue microarray construction and immunohistochemistry

Tissue blocks from 107 patients with Fédération Internationale de Gynécologie et d'Obstétrique (FIGO) stage II to stage IV advanced ovarian or peritoneal cancer treated with primary tumor debulking by a gynecologic oncologist from the Section of Gynecologic Oncology, University of Chicago, between 1994 and 2005, were selected for the study after international review board approval was obtained. A tissue microarray (TMA) was assembled and demographic and histopathologic data were collected, as previously reported (12).

TMA slides were deparaffinized in xylene and hydrated with alcohol before being placed in 1%  $\text{H}_2\text{O}_2$ /5% milk blocking solution. Antigen unmasking was then performed by boiling the slides in 0.01 mol/L citrate (pH 6.0;  $\alpha_5$ -integrin) or 1 mmol/L Tris-EDTA (pH 9.0; E-cadherin). Incubation with the primary  $\alpha_5$ -integrin antibody (H-104, Santa Cruz) or E-cadherin (4A2C7, Zymed) was done with a 1:200 dilution at 4°C overnight. After washing with TBS, the slides were stained using the Envision system. Immunohistochemical reactivity was scored independently without knowledge of clinical outcomes by two experienced pathologists (M.T.

and A.M.) as described before (18,19). Each sample was scored based on the percentage of positive cells (0,  $\leq 10\%$ ; 1, 10–25%; 2, 25–50%; 3,  $\geq 50\%$ ) and the intensity of the staining (0, none; 1, weak; 2, strong; representative samples are shown in Fig. 5). Only the samples which had strong staining of  $\alpha_5$ -integrin (intensity 2) in  $\geq 50\%$  of tumor cells (score 3) were considered as tumors overexpressing  $\alpha_5$ -integrin. Expression was considered “low” if the staining intensity was weak or 0 and/or  $< 50\%$  of all tumor cells were positive for  $\alpha_5$ -integrin. Endothelial cells constitutively express  $\alpha_5$ -integrin (20) and served as an internal positive control.

Specimens of normal human omentum were obtained from patients undergoing surgery for benign conditions. Omentum was stained with monoclonal fibronectin antibody (IST-4, Sigma) at a 1:600 dilution after antigen unmasking with 1 mmol/L Tris-EDTA (pH 8.0).

### Statistical analysis

Overall and progression-free survival estimates were computed using the Kaplan-Meier method, and comparisons between groups were analyzed using the log-rank test. Univariate analysis and multivariable models were fit using a Cox proportional hazards regression model. A backward elimination approach was used to fit the multivariable model so that variables achieving significance at the  $\alpha = 0.05$  level would be included. A large sample binomial test was conducted to determine whether the proportion positive for E-cadherin is equal to 0.5. A Spearman rank correlation test was conducted between normalized  $\alpha_5$ -integrin and E-cadherin expression at the  $\alpha = 0.05$  level.

## Results

### Down-regulation of E-cadherin up-regulates $\alpha_5$ -integrin and induces adhesion/invasion

To determine if E-cadherin loss affects expression of adhesion receptors that mediate cell-ECM interactions, an endogenously high E-cadherin expressing epithelial ovarian cancer cell line, RMUG-S, was transfected with an siRNA directed against E-cadherin (11). The surface expression of integrins and of the hyaluron receptor, CD44, were then measured by fluorescence-activated cell sorting (FACS). Although CD44 and several  $\alpha$ -integrins and  $\beta$ -integrins are expressed on RMUG-S cells, only  $\alpha_5$ -integrin expression was significantly up-regulated upon inhibition of E-cadherin (Fig. 1A). Immunoblotting confirmed that the E-cadherin specific siRNA down-regulates E-cadherin expression and corroborated the FACS data that E-cadherin inhibition induces  $\alpha_5$ -integrin expression (Fig. 1B). E-cadherin inhibition was specific, because it did not affect  $\beta_3$ -integrin or actin expression. The scrambled siRNA did not have an effect on E-cadherin or  $\alpha_5$ -integrin expression. Increased  $\alpha_5$ -integrin levels after E-cadherin inhibition in RMUG-S cells were a direct consequence of increased transcription, because inhibition of E-cadherin led to an increase in  $\alpha_5$ -integrin mRNA (Fig. 1C) and  $\alpha_5$ -integrin promoter activity (Fig. 1D).

To determine if E-cadherin and  $\alpha_5$ -integrin expressions are correlated, we measured E-cadherin and  $\alpha_5$ -integrin expression by Western blotting in eight additional ovarian cancer cell lines. Four cell lines (SKOV-3ip1, A2780, HeyA8, and OVMZ-6) expressed high levels of  $\alpha_5$ -integrin, whereas three (CAOV-3, OVCAR-5, RMUG-S) expressed high levels of E-cadherin. RMUG-L cells expressed equal amounts of E-cadherin and  $\alpha_5$ -integrin (Fig. 2A). Densitometric analysis indicated an inverse correlation between  $\alpha_5$ -integrin and E-cadherin (Pearson,  $R = -0.66$ ;  $P = 0.05$ ), and immunohistochemical staining of paraffin-embedded cell lines confirmed these findings (Supplementary Fig. S1).

Because  $\alpha_5$ -integrin is part of the fibronectin receptor  $\alpha_5\beta_1$ -integrin, we hypothesized that inhibition of E-cadherin would increase cell adhesion to fibronectin. RMUG-S cells were

transfected with the E-cadherin inhibiting siRNA labeled with a red fluorescent marker, and cells adhering to fibronectin were quantified by measuring fluorescence intensity. Inhibition of E-cadherin increased attachment to the fibronectin matrix by 4.7-fold and to collagen fibrills by 1.7-fold, whereas attachment to vitronectin bound predominantly by the  $\alpha_v\beta_3$ -integrin was only induced 1.3-fold, and attachment to plastic was not affected (Fig. 2B). The binding to fibronectin and collagen I is consistent with the ability of  $\alpha_5$ -integrin to bind these two ECM proteins, but  $\alpha_5$ -integrin binds less efficiently to the RGD motif of collagen (21). Because adhesion is followed by invasion, we then determined whether E-cadherin inhibition also induces invasion. E-cadherin siRNA-transfected RMUG-S cells invaded the Matrigel ECM efficiently, whereas cells transfected with the scrambled siRNA were significantly less invasive. The invasion into Matrigel could be partially inhibited with an  $\alpha_5\beta_1$ -integrin-blocking (IIA1; ref. 22) antibody (Fig. 2C). These results suggest that  $\alpha_5$ -integrin plays a key role in mediating both adhesion and invasion when E-cadherin is down-regulated. The effect of the IIA1 antibody is specific, because it blocked adhesion to fibronectin in  $\alpha_5$ -integrin over-expressing ovarian cancer cells (SKOV-3ip1) but not in  $\alpha_5$ -integrin-negative cells (RMUG-S) and did not inhibit adhesion to other ECM components, such as collagen, laminin, and vitronectin. Adhesion to fibronectin was blocked in a concentration-dependent manner (Supplementary Fig. S2).

### Inhibition of E-cadherin activates mitogen-activated protein kinase signaling

Next, we analyzed how down-regulation of E-cadherin induces  $\alpha_5$ -integrin, starting with signaling pathways known to be involved in E-cadherin signaling. Loss of E-cadherin liberates  $\beta$ -catenin, allowing for its nuclear translocation where it is a coactivator on promoters binding TCF/LEF transcription factors (3). Therefore,  $\beta$ -catenin expression and colocalization were analyzed. In RMUG-S cells, inhibition of E-cadherin leads to cytoplasmic localization but minimal nuclear translocation of  $\beta$ -catenin, as determined by confocal microscopy (Fig. 3A). Moreover, inhibition of E-cadherin did not activate  $\beta$ -catenin-dependent transcription of a promoter driven by three consecutive TCF transcription factor binding sites (Fig. 3B). These data suggest that in RMUG-S cells, inhibition of E-cadherin does not activate  $\beta$ -catenin-mediated transcriptional signaling.

Loss of E-cadherin can activate other signaling cascades, including mitogen-activated protein kinase (MAPK) and phosphatidylinositol 3-kinase (PI3K; ref. 4), which also play a role in ovarian cancer metastasis. Transfection with the E-cadherin siRNA (transfection efficiency, 80%) up-regulated  $\alpha_5$ -integrin and induced phosphorylation of FAK and Erk1-MAPK, whereas total levels of FAK and Erk1-MAPK were unchanged (Fig. 3C, left). In contrast, phosphorylation of p38-MAPK or c-Jun-NH<sub>2</sub>-kinase-MAPK was not affected by E-cadherin inhibition, nor was the PI3K signaling pathway, given that Akt phosphorylation was unchanged (Fig. 3C, left). To evaluate the role of FAK and Erk1 on  $\alpha_5$ -integrin induction, we overexpressed FAK and Erk1 and found that, when an expression plasmid for FAK or Erk1 was transfected into RMUG-S cells,  $\alpha_5$ -integrin was up-regulated (Fig. 3C, right). However, overexpression of p38 had no effect on  $\alpha_5$ -integrin.

Recently, a direct interaction between E-cadherin and the epidermal growth factor (EGF) receptor (EGFR) was described (22). In addition, loss of E-cadherin permits for ligand-dependent activation of EGFR (23). Given our data that loss of E-cadherin activates  $\alpha_5$ -integrin, we asked whether treatment with tyrphostin AG1478, an EGFR inhibitor, would affect  $\alpha_5$ -integrin expression. Treatment of E-cadherin siRNA transfected cells with tyrphostin blocked the up-regulation of  $\alpha_5$ -integrin observed after E-cadherin inhibition, whereas DMSO, the solvent for tyrphostin, had no effect (Fig. 3D, left). Confirming the role of EGFR in  $\alpha_5$ -integrin regulation, we found that stimulation of RMUG-S cells with EGF induced  $\alpha_5$ -integrin protein expression; an effect that could be partially inhibited with the Erk1-MAPK inhibitor PD 098059

(Fig. 3D, right). Therefore, whereas the increase in  $\alpha_5$ -integrin upon E-cadherin loss does not seem attributable to changes in  $\beta$ -catenin signaling, it is clearly associated with the activation of an EGFR/FAK/Erk-MAPK-dependent signaling pathway.

### An $\alpha_5\beta_1$ -integrin antibody inhibits adhesion and peritoneal metastasis

The data thus far indicate that  $\alpha_5$ -integrin is up-regulated upon E-cadherin loss and induces adhesion and invasion *in vitro*. To determine if this process is significant in human ovarian cancer metastasis, we first established that the  $\alpha_5\beta_1$ -integrin ligand fibronectin is present in human peritoneum (not shown) and omentum. All eight normal omental biopsies showed strong expression for extracellular fibronectin, which was present both in the submesothelial basement membrane and in the ECM surrounding omental fibroblasts and adipocytes (Supplementary Fig. S3A). Because the antibody used for the immunohistochemistry does not recognize intracellular FN and because a single layer of mesothelial cells cover the basement membrane of the omentum and peritoneum, a Western blot for fibronectin was performed after isolating primary human mesothelial cells covering the omentum. The results show that mesothelial cells express fibronectin and that they lay down a fibronectin-rich ECM (Supplementary Fig. S3B and C). Because the first step of ovarian cancer metastasis is adhesion to mesothelial cells covering the omentum and all internal organs, adhesion of SKOV-3ip1 cells to a three-dimensional culture and to the abdominal cavity of nude mice was determined. The three-dimensional culture, which is assembled from primary human mesothelial cells and fibroblasts extracted from human omentum, allows for the study of the early steps of omental metastasis (15). Incubation of SKOV3ip1 cells with the  $\alpha_5\beta_1$ -integrin-blocking antibody IIA1 partially inhibited cancer cell attachment to the three-dimensional culture, whereas incubation with blocking antibodies against  $\alpha_v\beta_3$ -integrin,  $\alpha_v\beta_5$ -integrin,  $\alpha_v\beta_6$ -integrin, and  $\beta_3$ -integrin had no effect (Supplementary Fig. S4A). At this point, short-term *in vivo* adhesion was evaluated after injection of cancer cells into the peritoneal cavity of nude mice. Untreated SKOV-3ip1 cells attached to the mouse peritoneum and omentum efficiently, whereas cells treated with IIA1 showed a 48% decrease in peritoneal attachment when compared with control IgG (Supplementary Fig. S4B).

Given that blocking  $\alpha_5$ -integrin inhibited adhesion and invasion, we examined the therapeutic potential of blocking  $\alpha_5$ -integrin in SKOV-3ip1 xenografts, an orthotopic model of advanced ovarian cancer. To simulate the clinical scenario, treatment was started 8 days after tumor cell injection, by which time the cells had metastasized and grown on mesothelial cell-coated abdominal surfaces (bowel mesentery, peritoneum, diaphragm, omentum). IgG-treated mice showed multiple tumors on the peritoneal surface, the omentum, the small bowel mesentery, and on both ovaries. The tumor burden was significantly higher ( $P < 0.05$ ) in the IgG-injected mice than in the IIA1 ( $\alpha_5$ -integrin-blocking antibody)-treated group, and the response was dose-dependent (Fig. 4A) as gauged by ascites volume, metastatic number, and tumor weight (tumor weight: IgG,  $1.34 \pm 0.39$  g; IIA1 10 mg,  $0.39 \pm 0.16$  g; IIA1 25 mg,  $0.22 \pm 0.20$  g). IIA1 inhibited the number of intraabdominal metastases; mice treated with IgG had significantly more tumor nodules (IgG,  $115 \pm 23.8$  lesions; IIA1 10 mg,  $46 \pm 15.4$  lesions; IIA1 25 mg,  $23.8 \pm 18.8$  lesions). The formation of ascites was blocked by 90% (10 mg) or 97% (25 mg), whereas the abdominal circumference of the mice treated with IgG was notably increased by ascites.

Staining of i.p. tumor nodules for CD31 expression (Fig. 4B) showed no differences between the three groups, suggesting that  $\alpha_5\beta_1$ -integrin inhibition on the cancer cells did not affect angiogenesis, which is consistent with the fact that the IIA1 antibody does not cross-react with mouse  $\alpha_5\beta_1$ -integrin. This was confirmed *in vitro* because expression of vascular endothelial growth factor protein was very similar in SKOV-3ip1 cells treated with IIA1 (data not shown).



IIA1-treated mice not only had fewer metastases, but the tumor nodules that did grow were much smaller than those found in control-treated mice, suggesting that the antibody has an antiproliferative effect. Indeed, staining of i.p. tumor nodules with the proliferation marker Ki-67 showed significant differences in antiproliferative effects between control-treated and IIA1-treated tumors ( $67.4 \pm 13.9\%$  versus  $33.6 \pm 15.5\%$  Ki-67-positive cells; Fig. 4B). Because Ki-67 staining reflects only the proliferation index at one time point, which is the end of the experiment, we sought to confirm this result *in vitro*. Treatment of SKOV-3ip1 cells with IIA1 clearly blocked proliferation over a 4-day culture period (Fig. 4B, right). A similar result was obtained with HeyA8 cells (not shown). To understand how blocking of  $\alpha_5$ -integrin reduced invasion, we analyzed protease activity using substrate zymograms. Treatment of SKOV-3ip1 with IIA1 blocked MMP9 gelatinolytic activity, whereas it had no effect on MMP2 or urokinase-associated proteolytic activity. In IIA1-treated tumors, the MMP-9 expression was significantly lower (Fig. 4C).

Based on these results, we performed a survival study with 10 mice in each group after i.p. injection of SKOV-3ip1 (Fig. 4D). Treatment (twice a week) with IIA1 was started after 8 days. Mice treated with the control IgG showed distress after an average of 37 days ( $\pm 1.3$ ), which is comparable with the life span of untreated mice injected with SKOV-3ip1 cells (12). Treatment of mice with the  $\alpha_5\beta_1$ -integrin antibody increased the median survival of inoculated mice by 12 days ( $49 \pm 4.8$  days, log rank;  $P < 0.0005$ ). The significant benefit of IIA1 treatment on survival was confirmed in a second ovarian xenograft model using the HeyA8 ovarian cancer cell line (not shown).

### **$\alpha_5$ -Integrin overexpression as a prognostic marker in ovarian cancer**

In view of the encouraging mouse experiments, which showed that blocking  $\alpha_5$ -integrin reduces tumor burden, we sought to determine if  $\alpha_5$ -integrin is expressed in human ovarian cancer.  $\alpha_5$ -Integrin protein expression was evaluated by immunohistochemistry on a TMA (Fig. 5A) with 107 patients (Table 1) with metastatic/advanced ovarian cancer (FIGO stages II–IV), all of whom underwent primary debulking followed by adjuvant chemotherapy. A section was considered positive when  $>50\%$  of all tumor cells were stained for  $\alpha_5$ -integrin, in accordance with a previous report on  $\alpha_5$ -integrin staining in lung cancer (24). A total of 42 patients (39%) were positive for  $\alpha_5$ -integrin. Among these positive cases, a tumor was considered to show overexpression when the staining intensity was evaluated as strong (score 2; Fig. 5A) by two independent pathologists. Strong staining was associated with 10 patients (9%), 6 of 81 with serous, 3 of 10 with clear cell, and 1 of 13 with endometrioid cancers. Median overall survival for patients with  $\alpha_5$ -integrin overexpression was 26 months versus 35 months for these with low or negative integrin expression ( $P = 0.03$ ).  $\alpha_5$ -Integrin was also a predictor of progression-free survival ( $P = 0.03$ ; Fig. 5B). Of the traditional markers of tumor aggressiveness, the size of the residual tumor left at the end of surgery, and ascites volume were statistically significant predictors of overall and progression-free survival (Table 1), as has been previously reported (2,12). For a multivariate analysis, a backwards elimination approach was used to select a model for overall survival with multiple predictors. Stage, histology, disease site, grading, residual disease, age, and  $\alpha_5$ -integrin expression were entered in this model. The final model included the size of the residual tumor and the level of  $\alpha_5$ -integrin expression as significant predictors for overall survival ( $P = 0.03$  and  $P = 0.04$ ). Because E-cadherin can regulate  $\alpha_5$ -integrin expression in ovarian cancer cell lines, we finally asked if tumors with high E-cadherin expression had low  $\alpha_5$ -integrin expression. We stained the tissue array for E-cadherin and quantified its expression as described for  $\alpha_5$ -integrin. In the cohort of 104 patients (three cores were missing in the TMA stained for E-cadherin), 20 patients had high E-cadherin expression (2+ staining). A binomial test of whether the proportion who were negative for  $\alpha_5$ -integrin was 0.5 was statistically significant ( $P = 0.014$ ). This suggests that

within the subgroup of E-cadherin-positive tumors, most (16 of 20) ovarian tumors are  $\alpha_5$ -integrin negative.

## Discussion

The goal of this study was to determine whether and how loss of E-cadherin affects expression of any of the adhesion receptors that mediate cell-ECM interactions and if the altered expression of this receptor(s) is important for ovarian cancer metastasis. Our experiments built on previous evidence that loss of E-cadherin is a frequent event in ovarian cancer and that it promotes peritoneal dissemination (5,25,26). Ovarian cancer cells in ascites fluid, as well as peritoneal implants, show markedly reduced expression of E-cadherin (5). Our data provide a novel mechanism by which loss of E-cadherin may promote metastasis in ovarian cancer. Upon E-cadherin down-regulation,  $\alpha_5$ -integrin is up-regulated and increases the ability of cancer cells to adhere to the mesothelial cells lining the abdominal cavity. These findings extend those of previous studies, which emphasize the important role of the  $\alpha_5$ -integrin/fibronectin interaction for the adhesion of ovarian cancer cells to the mesothelium (27,28). For example, Strobel et al. (28) showed that  $\alpha_5\beta_1$ -integrin expressed on ovarian cancer cells supports attachment of ovarian cancer cells to mesothelial cells. Casey et al. (29) reported that formation of ovarian cancer spheroids is mediated by  $\alpha_5\beta_1$ -integrin and fibronectin and that their adhesion can be inhibited with an  $\alpha_5$ -integrin antibody. Lastly, transformation of normal mammary epithelial cells with Ha-Ras induces  $\alpha_5$ -integrin and deposition of a fibronectin-rich ECM (30). The combined evidence from these studies suggests that loss of the cell-cell adhesion molecule E-cadherin induces cell-ECM adhesion through  $\alpha_5$ -integrin, which is consistent with the hypothesis that loss of E-cadherin induces a cascade of invasion and metastasis (3,4), whereas the presence of E-cadherin inhibits protease-mediated adhesion and invasion (31).

Ovarian cancer cells initially attach to mesothelial cells. We and others have shown that, several hours after the attachment of ovarian cancer cells, mesothelial cells focally begin to retract and detach (15,32). This is believed to be induced by FasL, which is secreted by cancer cells, and then binds to Fas receptors on mesothelial cells, thereby inducing apoptosis of the mesothelial cell (33). Expression of  $\alpha_5$ -integrin by cancer cells could provide them with a selection advantage, because it allows the ovarian cancer cells to attach to fibronectin secreted by mesothelial cells and then, upon the demise of the mesothelial cells, to attach to fibronectin present in the submesothelial basement membrane (Supplementary Fig. S3).

We provide evidence that E-cadherin regulates  $\alpha_5$ -integrin through an EGFR/FAK/Erk1-dependent signaling pathway and not through the canonical  $\beta$ -catenin pathway. E-cadherin loss did not change TCF-dependent transcription and  $\beta$ -catenin did not translocate to the nucleus upon E-cadherin inhibition, indicating that the adhesion modulating activity of E-cadherin is independent of  $\beta$ -catenin regulation of target gene(s). Wnt-independent signaling of E-cadherin was also reported in breast and prostate cancer cell lines, in which the expression of E-cadherin inhibited invasion independent of  $\beta$ -catenin/TCF signaling, but the pathway involved was not identified (34). In our studies, FAK and Erk1-MAPK are phosphorylated upon E-cadherin loss, indicating activation of the MAPK pathway. Consistent with MAPK activation, EGF induced  $\alpha_5$ -integrin expression and inhibition of EGFR with tyrphostin abrogated the induction of  $\alpha_5$ -integrin by E-cadherin. These findings are consistent with reports that confluent, adherence junction rich cells show no EGFR activity (23,35). Quian et al. (35) established that expression of E-cadherin leads to inactivation of the EGFR through direct interaction with E-cadherin, thereby altering the ligand-binding site within EGFR, which results in the inability of EGF to stimulate EGFR. Therefore, we propose a mechanism whereby loss of E-cadherin frees EGFR from repression by the adhesion molecule, allowing for EGF regulation of  $\alpha_5$ -integrin through the MAPK pathway.

We have identified  $\alpha_5$ -integrin as a marker of aggressive ovarian cancer. Analysis of the clinical data revealed that elevated expression of  $\alpha_5$ -integrin is linked to significantly reduced survival. Hazard ratio analysis confirmed that  $\alpha_5$ -integrin is a stand alone variable and indicated that high expression of this integrin is an independent risk factor for patient survival, similar in significance to the amount of residual tumor at the completion of tumor debulking, which is a well known prognostic factor (2,12). Although only a subgroup of patients overexpress  $\alpha_5$ -integrin, 39% of all ovarian cancer tumors express  $\alpha_5$ -integrin. These are the first results describing  $\alpha_5$ -integrin expression in ovarian cancer and are similar to findings by Adachi et al. (24) that 49% of all lung cancers express  $\alpha_5$ -integrin and that patients with  $\alpha_5$ -integrin expression have significantly lower overall survival.

Our results show that  $\alpha_5\beta_1$ -integrin inhibition with a blocking antibody is effective both *in vitro* and *in vivo* and identify  $\alpha_5$ -integrin as a new target in ovarian cancer treatment. IIA1 inhibited invasion upon E-cadherin down-regulation and specifically reduced adhesion to fibronectin, as well as to a three-dimensional culture of omental metastasis. Inhibition of  $\alpha_5\beta_1$ -integrin also reduced initial tumor cell attachment to mouse omentum and peritoneum in a manner similar to that observed *in vitro*. Furthermore, in addition to its effects on adhesion and invasion, the antibody also exhibits antiproliferative activity and inhibits MMP9 gelatinolytic activity, which explains its effect on established tumors. These four mechanisms (inhibition of adhesion, invasion, proliferation, MMP-9 activity) are certainly, at least partially, responsible for the ability of  $\alpha_5$ -integrin inhibition to increase animal survival in two xenograft models (SKOV-3ip1 and HeyA8) by an average of 10 days, as well as reduce tumor load and the number of metastasis. The antibody used in this study to block  $\alpha_5\beta_1$ -integrin (IIA1) does not cross-react with mouse  $\alpha_5\beta_1$ -integrin (22), and therefore, the inhibitory effects reported here are necessarily a result of the direct inhibition of  $\alpha_5\beta_1$ -integrin in the human cell lines. As expected, the vessel density was similar in all treatment groups because of the selectivity of IIA1 for human  $\alpha_5\beta_1$ -integrin. Still, an important role for  $\alpha_5\beta_1$ -integrin in angiogenesis has been clearly established (36,37). We have recently shown that a human-mouse chimeric version of IIA1 can inhibit tube formation in human umbilical chord endothelial cells and also induce apoptosis in proliferating endothelial cells (38). In a cynomolgus model of choroidal neovascularization, the antibody inhibited angiogenesis with no obvious toxicities (38). Given the antiangiogenic effects of  $\alpha_5\beta_1$ -integrin inhibition (36,37), blocking this integrin on human endothelial and tumor cells may possibly result in even greater therapeutic efficacy through the combination of antiangiogenic and antitumoral effects.

The role of  $\alpha_5\beta_1$ -integrin as a potential anticancer target has recently attracted some interest. Blocking  $\alpha_5\beta_1$ -integrin mediated cell adhesion with a small molecule antagonist (SJ479) in two human astrocytoma cell lines reduced soft agar growth and blocked proliferation (39). Also, a fibronectin-derived peptide that blocks the interaction of  $\alpha_5\beta_1$ -integrin with fibronectin inhibited invasion, angiogenesis, and metastasis in prostate and colon cancer models (40,41). Ovarian cancer may be especially suited to an  $\alpha_5$ -integrin-targeting approach due to its unique tumor biology, which is initially dependent on attachment to a fibronectin-rich mesothelial surface. Therefore, in light of multiple publications, highlighting the importance of  $\alpha_5$ -integrin in tumor biology (39–41) and the results described here, we are supportive of clinical trials studying whether anti  $\alpha_5$ -integrin treatment is a viable treatment strategy in ovarian cancer.

## Supplementary Material

Refer to Web version on PubMed Central for supplementary material.

## Acknowledgments

**Grant support:** Ovarian Cancer Research Fund (Liz Tilberis Scholars Program) and NIH grant R01 CA111882 (to E. Lengyel). PDL provided funding for the animal experiments.

We thank Dr. Ritzenthaler (Emory University, Atlanta, GA) for providing us with the  $\alpha 5$ -integrin promoter constructs. We thank Dr. Sanford Shattil (Division of Hematology-Oncology, UCSD) and Dr. George VandeWoude (Van Andel Institute) for helpful suggestions. We greatly appreciate Gail Isenberg for editing the manuscript.

## References

1. Auersperg N, Wong AST, Choi K, et al. Ovarian surface epithelium: biology, endocrinology and pathology. *Endocr Rev* 2001;22:255–288. [PubMed: 11294827]
2. Cannistra SA. Cancer of the ovary. *N Engl J Med* 2004;351:2519–2529. [PubMed: 15590954]
3. Huber MA, Kraut N, Beug H. Molecular requirements for epithelial-mesenchymal transition during tumor progression. *Curr Opin Cell Biol* 2006;17:548–558. [PubMed: 16098727]
4. Cavallaro U, Christofori G. Cell adhesion and signalling by cadherins and IG-cams in cancer. *Nat Rev* 2004;4:118–132.
5. Veatch AL, Carson LF, Ramakrishnan S. Differential expression of the cell-cell adhesion molecule E-cadherin in ascites and solid human ovarian tumor cells. *Int J Cancer* 1994;58:393–399. [PubMed: 7519585]
6. Darai E, Scoazec JY, Walker-Combrouze F, et al. Expression of cadherins in benign, borderline, and malignant ovarian epithelial tumors: a clinicopathologic study of 60 cases. *Hum Pathol* 1997;28:922–928. [PubMed: 9269828]
7. Symowicz J, Adley BP, Gleason KJ, et al. Engagement of collagen-binding integrins promotes matrix metalloproteinase-9-dependent E-cadherin ectodomain shedding in ovarian carcinoma cells. *Cancer Res* 2007;67:2030–2039. [PubMed: 17332331]
8. Cannistra SA, Kansas GS, Niloff J, et al. Binding of ovarian cancer cells to peritoneal mesothelium *in vitro* is partly mediated by CD44H. *Cancer Res* 1993;53:3830–3838. [PubMed: 8339295]
9. Ahmed N, Riley C, Oliva K, et al. Ascites induces modulation of  $\alpha 6 \beta 1$  integrin and urokinase plasminogen activator receptor expression and associated functions in ovarian carcinoma. *Br J Cancer* 2005;92:1475–1485. [PubMed: 15798771]
10. Sawada M, Shii J, Akedo H, et al. An experimental model for ovarian tumor invasion of cultured mesothelial cell monolayer. *Lab Invest* 1994;70:333–338. [PubMed: 8145527]
11. Le Floch A, Jalil A, Vergnon I, et al.  $\alpha E \beta 7$  integrin interaction with E-cadherin promotes antitumor CTL activity by triggering lytic granule polarization and exocytosis. *J Exp Med* 2007;204:559–570. [PubMed: 17325197]
12. Sawada K, Radjabi AR, Shinomiya N, et al. C-Met overexpression is a prognostic factor in ovarian cancer and an effective target for inhibition of peritoneal dissemination and invasion. *Cancer Res* 2007;67:1670–1680. [PubMed: 17308108]
13. Shell S, Park S, Radjabi AR, et al. Let-7 expression defines two differentiation stages of cancer. *Proc Natl Acad Sci U S A* 2007;104:11400–11405. [PubMed: 17600087]
14. Boles BK, Ritzenthaler J, Birkenmeier T, et al. Phorbol ester-induced U-937 differentiation: effects on integrin  $\alpha 5$  gene transcription. *Am J Physiol Cell Mol Physiol* 2000;278:703–712.
15. Kenny HA, Krausz T, Yamada SD, et al. Development of an organotypic peritoneal three-dimensional culture to study peritoneal attachment of ovarian cancer cells. *Int J Cancer* 2007;121:1463–1472. [PubMed: 17546601]
16. Lengyel E, Schmalfeldt B, Konik E, et al. Expression of latent matrix metalloproteinase 9 (MMP-9) predicts survival in advanced ovarian cancer. *Gynecol Oncol* 2001;82:291–298. [PubMed: 11531282]
17. Lengyel E, Wang H, Gum R, et al. Elevated urokinase-type plasminogen activator receptor expression in a colon cancer cell line is due to a constitutively activated extracellular-signal regulated kinase 1 dependent signaling cascade. *Oncogene* 1997;14:2563–2574. [PubMed: 9191056]

18. Lengyel E, Prechtel D, Resau JH, et al. C-Met overexpression in node-positive breast cancer identifies patients with poor clinical outcome independent of Her2/Neu. *Int J Cancer* 2005;113:678–682. [PubMed: 15455388]
19. Mell LK, Meyer JJ, Tretiakova MS, et al. Prognostic significance of E-cadherin protein expression in pathological stage I–III endometrial cancer. *Clin Cancer Res* 2004;10:5546–5553. [PubMed: 15328195]
20. Wingerter P, Kazman I, Norberg S, et al. Uniform overexpression and rapid accessibility of  $\alpha 5\beta 1$  integrin on blood vessels in tumors. *Am J Pathol* 2005;167:193–211. [PubMed: 15972964]
21. Hynes R. Integrins: versatility, modulation, and signaling in cell adhesion. *Cell* 1992;69:11–25. [PubMed: 1555235]
22. Nhieu G, Isberg R. Bacterial internalization mediated by  $\beta 1$  chain integrins is determined by ligand affinity and receptor density. *EMBO J* 1993;12:1887–1895. [PubMed: 8491181]
23. Hoschuetzky H, Aberle H, Kemler R.  $\beta$ catenin mediates the interaction of the cadherin-catenin complex with epidermal growth factor receptor. *J Cell Biol* 1994;127:1375–1380. [PubMed: 7962096]
24. Adachi A, Taki T, Higashiyama M, et al. Significance of integrin- $\alpha$  gene expression as a prognostic factor in node-negative non small cell lung cancer. *Clin Cancer Res* 2000;6:96–101. [PubMed: 10656437]
25. Yuecheng Y, Hongmei L, Xiaoyan X. Clinical evaluation of E-cadherin expression and its regulation mechanism in epithelial ovarian cancer. *Clin Exp Metastasis* 2006;23:65–74. [PubMed: 16826427]
26. Makarla PB, Saboorian MH, Ashfaq R, et al. Promoter hypermethylation profile of ovarian epithelial neoplasms. *Clin Cancer Res* 2005;11:5365–5369. [PubMed: 16061849]
27. Shibata K, Kikkawa F, Nawa A, et al. Fibronectin secretion from human peritoneal tissue induces Mr 92,000 type IV collagenase expression and invasion in ovarian cancer cell lines. *Cancer Res* 1997;57:5416–5420. [PubMed: 9393769]
28. Strobel T, Cannistra SA.  $\beta 1$ -integrins partly mediate binding of ovarian cancer cells to peritoneal mesothelium *in vitro*. *Gynecol Oncol* 1999;73:362–367. [PubMed: 10366461]
29. Casey RC, Burleson KM, Skubitz KM, et al.  $\beta 1$ -integrins regulate the formation and adhesion of ovarian carcinoma multicellular spheroids. *Am J Pathol* 2001;159:2071–2080. [PubMed: 11733357]
30. Maschler S, Wirl G, Spring H, et al. Tumor cell invasiveness correlates with changes in integrin expression and localization. *Oncogene* 2005;24:2032–2041. [PubMed: 15688013]
31. Munshi HG, Ghosh S, Mukhopadhyay S, et al. Proteinase suppression by E-cadherin-mediated cell-cell attachment in premalignant oral keratinocytes. *J Biol Chem* 2002;277:38159–38167. [PubMed: 12138162]
32. Niedbala MJ, Crickard K, Bernacki R. Interactions of human ovarian tumor cells with human mesothelial cells grown on extracellular matrix. *Exp Cell Res* 1985;160:499–513. [PubMed: 3899694]
33. Heath R, Jayne D, O’Leary R, et al. Tumor-induced apoptosis in human mesothelial cells: a mechanism of peritoneal invasion by Fas Ligand/Fas interaction. *Br J Cancer* 2004;90:1437–1442. [PubMed: 15054468]
34. Wong AST, Gumbiner BM. Adhesion-independent mechanism for suppression of tumor cell invasion by E-cadherin. *J Cell Biol* 2003;161:1191–1203. [PubMed: 12810698]
35. Qian X, Karpova T, Sheppard AM, et al. E-cadherin-mediated adhesion inhibits ligand-dependent activation of diverse receptor tyrosine kinases. *EMBO J* 2004;23:1739–1748. [PubMed: 15057284]
36. Kim S, Bell K, Mousa SA, et al. Regulation of angiogenesis *in vivo* by ligation of integrin  $\alpha 5\beta 1$  with the central cell-binding domain of fibronectin. *Am J Pathol* 2000;156:1345–1362. [PubMed: 10751360]
37. Magnussen A, Kasman I, Norberg S, et al. Rapid access of antibodies to  $\alpha 5\beta 1$  integrin overexpressed on the luminal surface of tumor blood vessels. *Cancer Res* 2005;65:2712–2721. [PubMed: 15805270]
38. Ramakrishnan V, Bhaskar V, Law DA, et al. Preclinical evaluation of an anti- $\alpha 5\beta 1$  integrin antibody as a novel anti-angiogenic agent. *J Exp Ther Oncol* 2007;5:273–286. [PubMed: 17024968]
39. Maglott A, Bartik P, Cosgun S, et al. The small  $\alpha 5\beta 1$  integrin antagonist, SJ749, reduces proliferation and clonogenicity of human astrocytoma cells. *Cancer Res* 2006;66:6002–6008. [PubMed: 16778170]

40. Stoeltzing O, Liu W, Reinmuth N, et al. Inhibition of integrin  $\alpha 5 \beta 1$  function with a small peptide (ATN-161) plus continuous 5-FU infusion reduces colorectal liver metastases and improves survival in mice. *Int J Cancer* 2003;104:496–503. [PubMed: 12584749]
41. Livant DL, Brabec RK, Pienta KJ, et al. Anti-invasive, antitumorigenic, and antimetastatic activities of the PHSCN sequence in prostate carcinoma. *Cancer Res* 2000;60:309–320. [PubMed: 10667582]

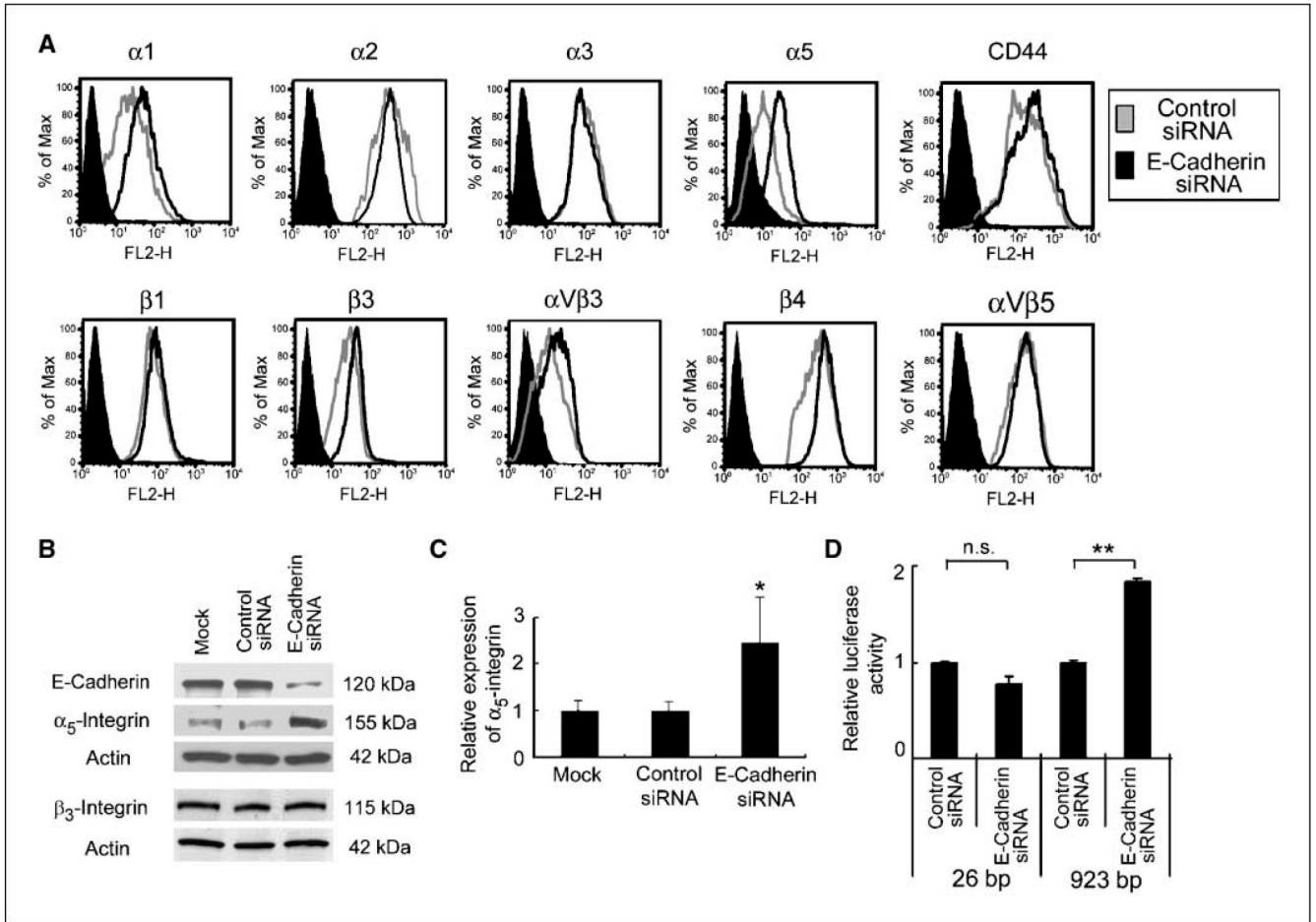


**Figure 1. Down-regulation of E-cadherin up-regulates  $\alpha 5$ -integrin**

A, the surface expression of adhesion receptors was evaluated by FACS. RMUG-S cells transfected with E-cadherin siRNA (black line) or control siRNA (gray line) were incubated with the primary antibody against  $\alpha 1$ -integrin,  $\alpha 2$ -integrin,  $\alpha 3$ -integrin,  $\alpha 5$ -integrin,  $\beta 1$ -integrin,  $\beta 3$ -integrin,  $\beta 4$ -integrin,  $\alpha \beta 3$ -integrin, or  $\alpha \beta 5$ -integrin, an antibody against CD44 and control IgG (filled black histogram), followed by a phycoerythrin conjugated secondary antibody. B, RMUG-S cells transfected with the E-cadherin siRNA, a control siRNA, or mock-transfected cells were harvested 96 h after transfection. Cell lysates were resolved by SDS-PAGE and immunoblotted with anti-E-cadherin, anti- $\alpha 5$ -integrin, and anti- $\beta 3$  antibody. The membrane was stripped and reprobed with  $\beta$ -actin. C, quantitative real-time RT-PCR. Total RNA was extracted from RMUG-S cells, and the relative expression of  $\alpha 5$ -integrin normalized to GAPDH was measured using Taqman quantitative real-time RT-PCR. D, effect of E-cadherin inhibition on  $\alpha 5$ -integrin promoter activity. After silencing E-cadherin, RMUG-S cells were transiently transfected with 1  $\mu$ g of -923 bp or the deleted -26 bp  $\alpha 5$ -integrin promoter luciferase construct. Luciferase activity was analyzed 48 h after transfection and standardized for *Renilla* luciferase activity. Columns, average value for three independent experiments; bars, SD. Significant differences are indicated by \* for  $P < 0.05$ , \*\* for  $P < 0.01$ , and n.s. for not significant.

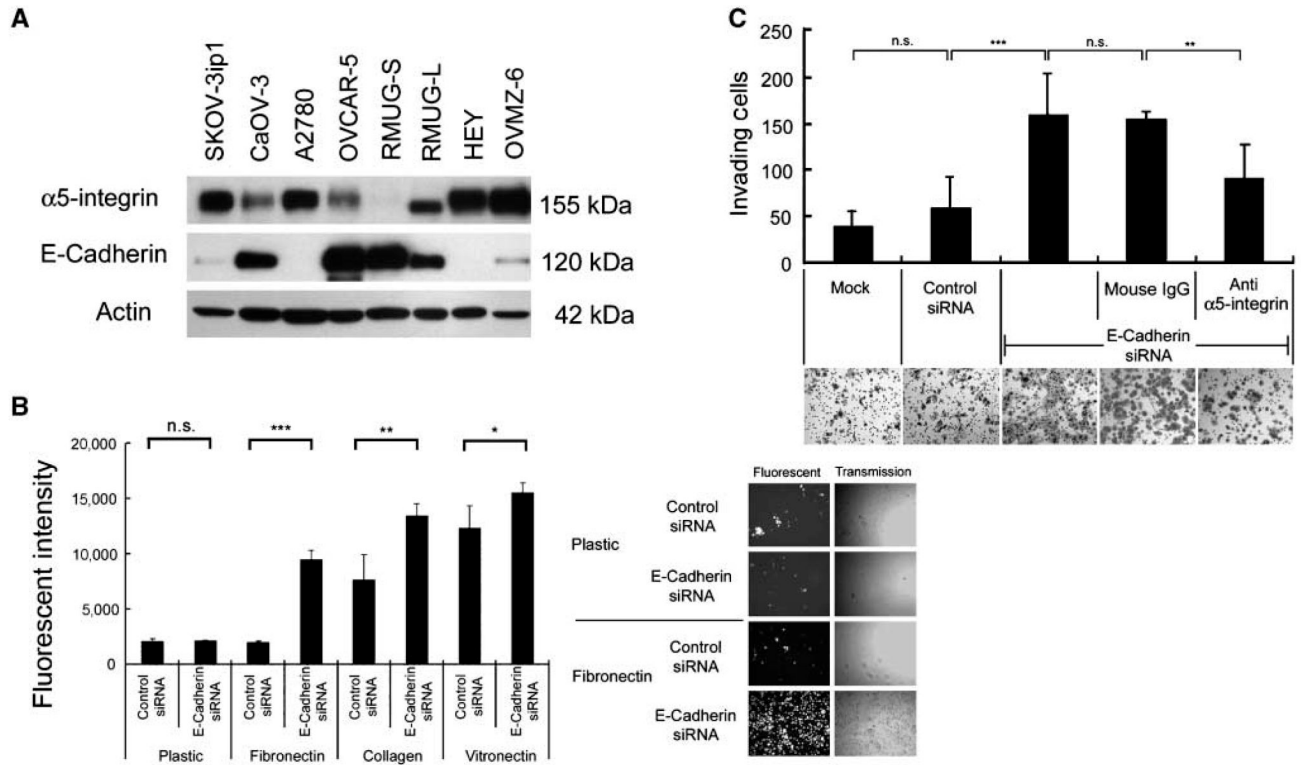


**Figure 2. Down-regulation of E-cadherin induces cell adhesion and invasion via up-regulation of  $\alpha 5$ -integrin**

*A*, Western blot. Cell lysates were resolved by SDS-PAGE and immunoblotted with an antibody against  $\alpha 5$ -integrin or E-cadherin. Blots are representative of three experiments. *B*, adhesion to ECM. E-cadherin- or control siRNA–transfected RMUG-S cells were fluorescently labeled and plated onto 96-well plates coated with the indicated ECM components. Plates were washed and the number of adherent cells was quantified by measuring fluorescence intensity. *Columns*, mean of three independent experiments. Representative images of labeled cells that have attached are in the right panel. *C*, invasion. RMUG-S cells were transfected with the E-cadherin siRNA or control siRNA or not transfected (mock). The transfected cells were placed in a Matrigel-coated Boyden chamber and allowed to invade for 24 h.  $\alpha 5$ -Integrin–blocking antibody (IIA1) or nonspecific mouse IgG was added as indicated. Representative photographs are shown. The results were from three independent experiments. Significant differences are indicated by \* for  $P < 0.05$ , \*\* for  $P < 0.01$ , \*\*\* for  $P < 0.001$ , and n.s. for not significant.



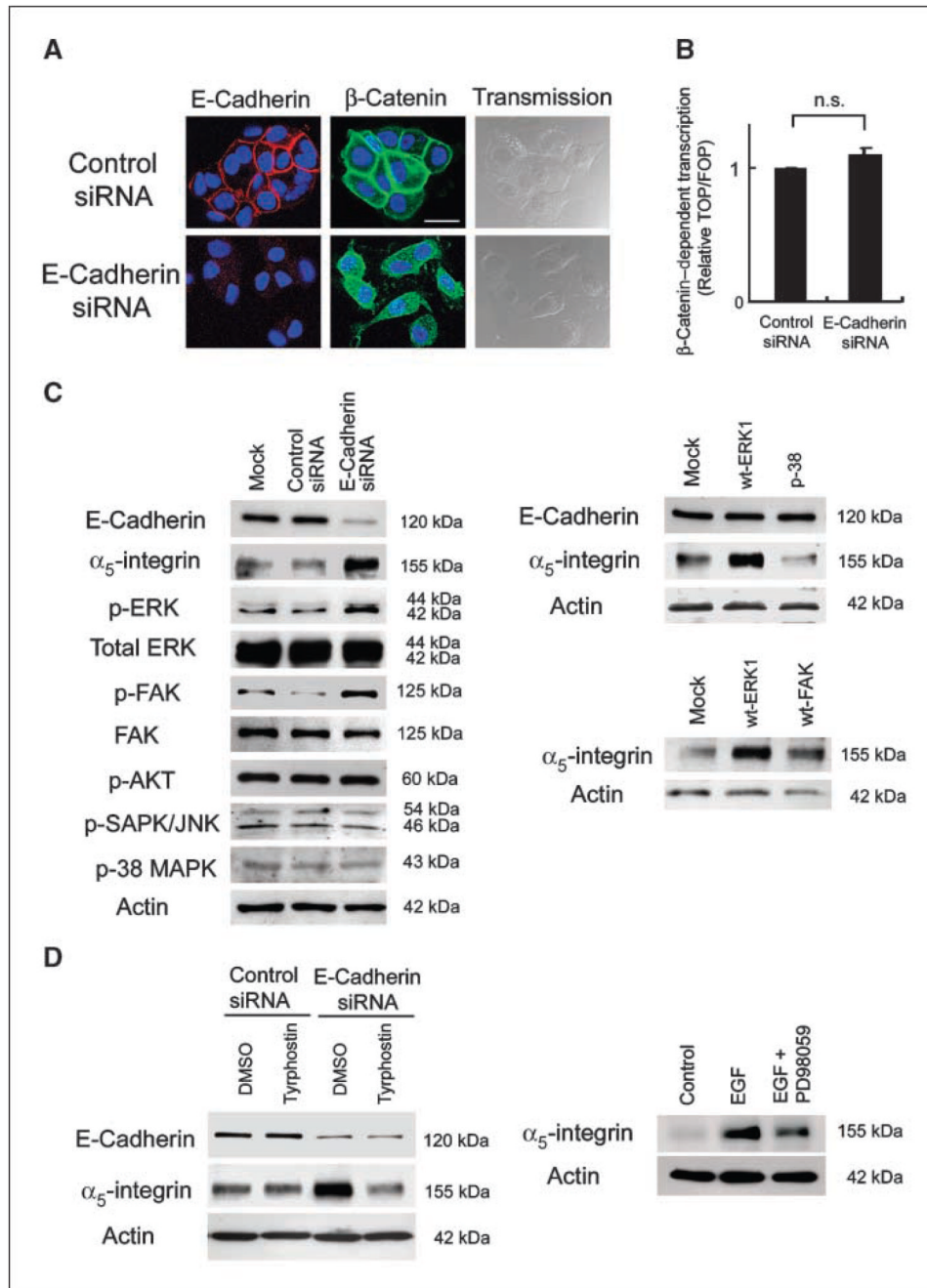


### Figure 3. Inhibition of E-cadherin activates MAPK signaling

**A**, confocal microscopy. Transfected RMUG-S cells were plated on chamber slides and stained with an E-cadherin or  $\beta$ -catenin antibody followed by Alexa Fluor 555 (red)- or Alexa Fluor 488 (green)- labeled secondary antibody and stained with DAPI. Bar, 20  $\mu$ m. **B**, transient transfection with a  $\beta$ -catenin-LEF/TCF reporter gene. RMUG-S cells were cotransfected with the E-cadherin siRNA and either TOPFLASH (four wt TCF binding sites) or FOPFLASH (four mutant TCF binding sites) firefly luciferase reporter. Luciferase activity was analyzed 48 h after transfection and normalized for *Renilla* luciferase activity. The results were from three independent experiments. *n.s.*, not significant. **C**, Western Blot. RMUG-S cells were transfected with the E-cadherin siRNA or control siRNA (*left*). Lysates were resolved by SDS-

PAGE and immunoblotted with the indicated antibodies. The experiments were repeated at least thrice. RMUG-S cells were transfected with an expression plasmid for wt-ERK1, wt-p38, or wt-FAK, lysed, and immunoblotted (*right*). The membrane was stripped and reprobed with  $\beta$ -actin as internal loading control. *D*, RMUG-S cells were transfected with the E-cadherin siRNA or a control siRNA and then treated with either Tyrphostin (10  $\mu$ mol/L) or the solvent DMSO (*left*). *Right*, RMUG-S cells were stimulated with EGF for 24 h or with EGF and the MAPK inhibitor PD098059; cells were lysed and immunoblotted with an  $\alpha_5$ -integrin antibody.

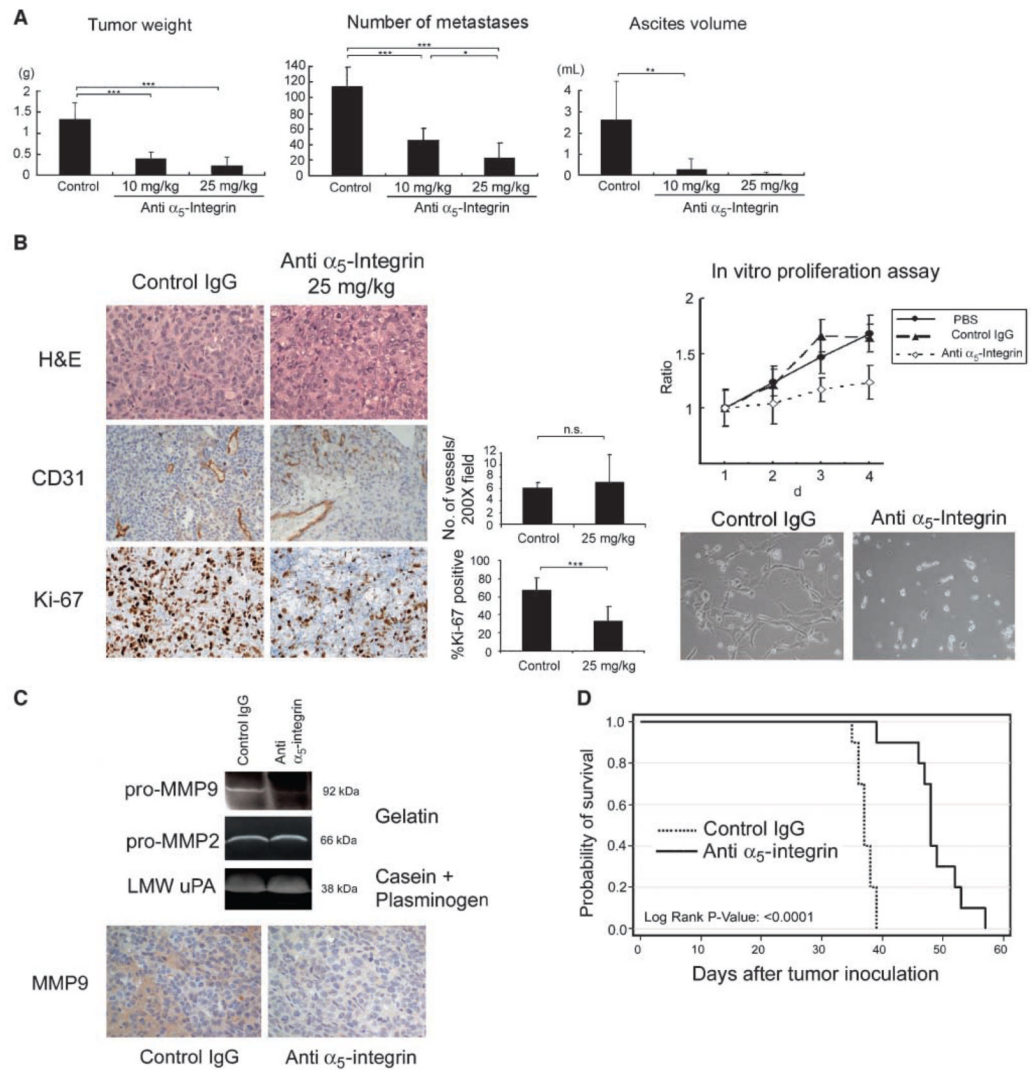


**Figure 4. Effects of the  $\alpha_5\beta_1$ -integrin antibody on an ovarian cancer xenograft model**

SKOV-3ip1 cells ( $1 \times 10^6$ ) were injected i.p. One week after injection, IIA1 antibody or nospecific mouse IgG was injected twice a week for a total of 4 wk of treatment. **A**, effects of IIA1 antibody on i.p. tumor weight, number of metastases, and ascites formation. **B**, *left*, representative tumor areas were stained with H&E, the angiogenesis marker CD31 ( $\times 200$ ), and the proliferation marker Ki-67 ( $\times 100$ ). *Middle*, the number of microvessels per field for CD31 and the percentage of Ki-67 positive nuclei. *Right*, Effects of IIA1 on the proliferation of ovarian cancer cells *in vitro*. SKOV3 ip1 cells were treated with the control mouse IgG or IIA1 antibody and proliferation measured using a fluorescent dye that incorporates into nucleic acids. **C**, *top*, zymogram. Cells were treated with IIA1, switched to serum-free medium, and a gelatin or casein/plasminogen zymogram was performed. *Bottom*, representative tumor areas were stained for MMP9 ( $\times 100$ ). **D**, SKOV3ip1 cells ( $1 \times 10^6$ ) were inoculated i.p. into nude mice ( $n = 10$ ) and after 8 d of treatment with IIA1 or control IgG started (twice a week) until the mice showed signs of distress. Kaplan-Meier survival curves were calculated. The IIA1 antibody significantly improved the overall survival of cancer-bearing mice ( $P < 0.0001$ ; log-rank test). *Columns*, mean; *bars*, SD. Significant differences are indicated by \* for  $P < 0.05$ , \*\* for  $P < 0.01$ , \*\*\* for  $P < 0.001$ , and n.s. for not significant.

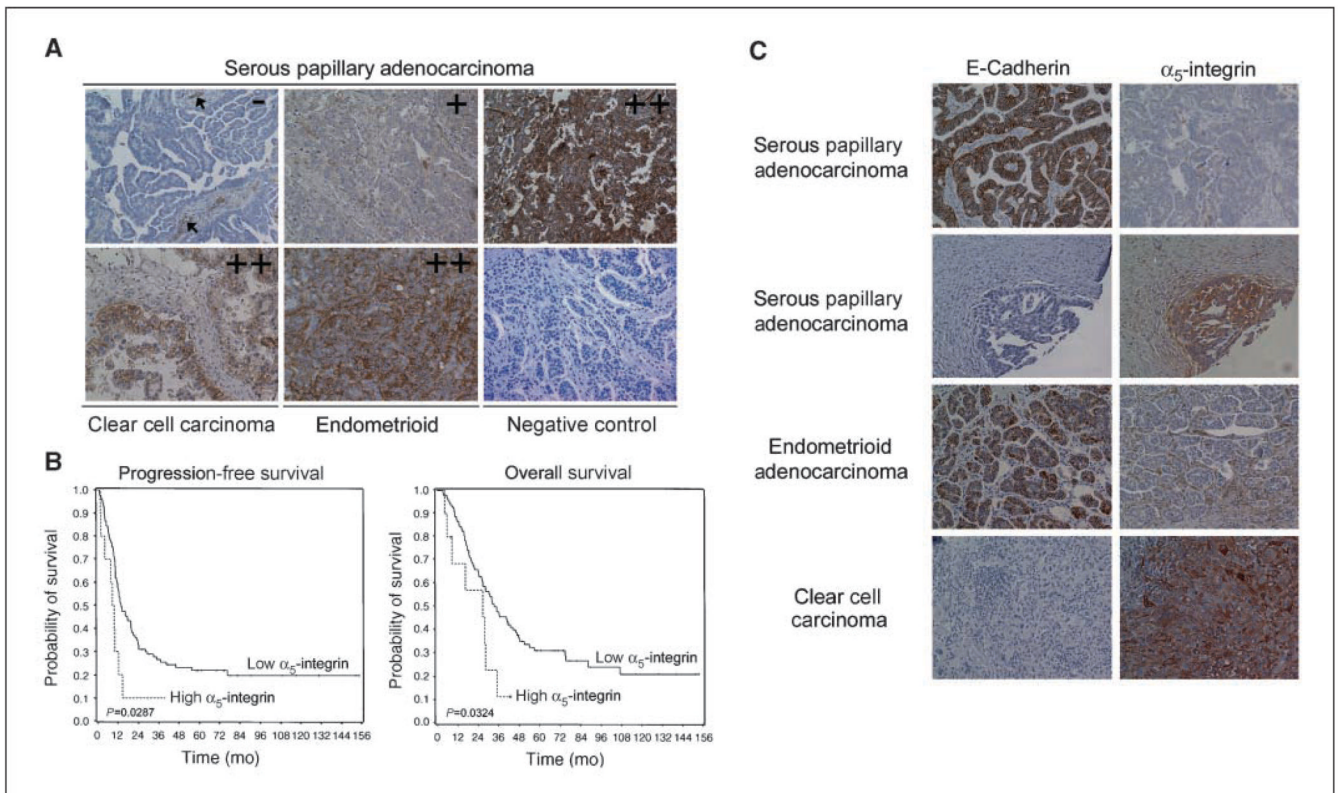


**Figure 5.  $\alpha_5$ -Integrin overexpression is a prognostic marker in ovarian cancer**

**A**, representative sections of different ovarian cancers stained using an antibody against human  $\alpha_5$ -integrin and scored as 0, 1, and 2+. The negative control is nonimmune sera; arrows show blood vessels, which served as an internal control. **B**, Kaplan-Meier curves of progression-free and overall survival in 107 patients with FIGO stages II to IV advanced ovarian cancer treated with primary surgery followed by chemotherapy with carboplatin and paclitaxel. **C**, E-cadherin or  $\alpha_5$ -integrin immunostaining of sequential sections from four different ovarian cancers. The photographs were taken at 200 $\times$  magnification.

**Table 1**Clinical data of patients with FIGO stage II–IV tumors ( $n = 107$ )

Median age, y (range)	59 (39–87)	<i>P</i> (progression-free survival)
Median observation time of patients alive, mo (range)	67 (8–153)	
FIGO Stage	<i>n</i> (%)	
IIC	8 (7.5)	0.2095
IIIA	3 (2.8)	
IIIB	2 (1.9)	
IIIC	69 (64.5)	
IV	25 (23.4)	
Histology		
Serous-papillary	81 (75.7)	0.0071
Endometrioid	13 (12.2)	
Clear cell	10 (9.4)	
Mucinous	3 (2.8)	
Disease		
Ovarian	99	
Primary peritoneal	7	
Primary fallopian tube	1	
Grading		
G1 + G2	26 (24.3)	0.6096
G3	81 (75.7)	
Ascites volume		
≤500 mL	43 (40.2)	0.0014
>500 mL	54 (50.5)	
Unknown	10 (9.3)	
Residual tumor		
≤1 cm	62 (57.9)	0.0191
>1 cm	43 (40.2)	
Unknown	2 (1.9)	
Chemotherapy type		
Adjuvant	107 (100.0)	
Chemotherapy		
Taxane/platinum	101 (94.3)	
Cytosin/platinum	3 (2.8)	
Platinum only	2 (1.9)	
Taxane	1 (0.9)	